ENCIT 2018

ABCM Associação Brasileira de Engenharia e Ciências Mecânicas

17th Brazilian Congress of Thermal Sciences and Engineering
November 25th-28th, 2018, Águas de Lindóia, SP, Brazil

ENCIT-2018-XXXX
APPLICATION OF THE SA OPTIMISATION METHOD TO THE CORRELATED WMP RADIATION MODEL FOR FLAMES

Bruno Hartmann da Silva
Isaias Mortari Machado
Fernando Marcelo Pereira
Francis Henrique Ramos França
Department of Mechanical Engineering, Federal University of Rio Grande do Sul, UFRGS, Porto Alegre, Rio Grande do Sul, Brazil
bruno.hartmann@ufrgs.br;
imortarim@gmail.com;
fernando@mecanica.ufrgs.br;
frfranca@ufrgs.br

Paulo Roberto Pagot
CENPES/PDEP/TPP - PETROBRAS, Petróleo Brasileiro S. A., Rio de Janeiro, Rio de Janeiro, Brazil
pagot@petrobras.com.br

Abstract. *The weighted-multi-point-source (WMP) model is an imminent alternative to detailed flame simulations when estimations of thermal radiation in both far and near fields are needed. However, despite its easier implementation, several parameters need to be set in order to guarantee the accuracy of the results. These parameters are still unknown and may depend on several variables, such as the fuel that is being burnt, the mass flow and the percentage of inert gas in the mixture. The large quantity of variables demands the use of an efficient method to determine these parameters based in experimental data. Previous studies used the Generalized Extremal Optimization (GEO) method to determine the best combinations of variables for the problem and correlate with flame parameters. This work aims to further explore the problem applying the well established Simulated Annealing (SA) algorithm and comparing the results to those offered by the GEO, assessing which is the best choice to the correlated WMP problem. It is used the same methodology of the compared paper, using a quadratic correlation between the variables (radiation fractions and sources weights) and the flame heat release rate. A total of 77 cases were studied and the results were analysed in a statistical study over 50 runs. The SA algorithm showed better results with similar average values of objective function, but lower best case values.*

Keywords: *WMP, inverse problem, combustion, optimisation, simulated annealing*

1. INTRODUCTION

The operation of combustion based processes require models that are capable to predict accurately the effect of thermal radiation emitted from flames. Several applications to these models are found in energy and oil industries, for instance boilers, furnaces, gas turbines, and flares used to burn rejected gases in refineries and oil offshore platforms. Nowadays this modelling in engineering practice is usually done using the single-point (SP) model, which is adequate for far field applications. However, for near field applications, the SP model is not capable to predict the radiation profile accurately since spatial effects, negligible for large distances from the flame, become more important as the point of interest gets closer to the source. For this reason, Hankinson and Lowesmith (2012) proposed and compared several flame modelling approaches, among them the weighted-multi-point-source (WMP) model, in order to obtain a radiation profile similar to that measured experimentally. In order to use the WMP model, however, many parameters must be determined. They can be formulated as functions of variables that characterize the flame, e.g. the heat release rate of the flame or its visible length. Depending on the chosen formulation, a large number of different solutions appear to solve de problem and it becomes difficult to determine if the solution is really the best one or just a local optimum.

There are several strategies to solve this type of multivariate problems. Deterministic methods, such as gradient descent, cannot be used with confidence, since they do not guarantee the encounter of the global minimum. Several stochastic methods were developed aiming to find the solution for these problems in a more efficient way. Among the most used are Particle Swarm Optimization - PSO (Kennedy and Eberhart (1995)), Artificial Bee Colony Algorithm (Lucic and Teodorovic (2001)) and genetic algorithms (Holland (1975)). The Simulated Annealing algorithm (Kirkpatrick *et al.* (1983)) is one of these methods largely implemented for its simplicity, despite being very sensible to change in

its parameters. Nevertheless, the standard SA algorithm as well as its variations have demonstrated to be effective in several engineering applications, as shown recently by Wei *et al.* (2018) (logistics planning), Fang *et al.* (2018) (image reconstruction) and Erchiqui (2018) (thermal processes optimisation). In fact, the stochastic computation strategy has already been applied by Miguel *et al.* (2016) to solve the correlated WMP problem, when the Generalized Extremal Optimisation (GEO) was used. However, since the GEO can have numeric resolution limitations and the behaviour of the problem is unknown, there is a chance that the results offered by the GEO method could be improved without losing computing efficiency and the SA algorithm could have potential to deliver these improvements as showed by the cited works.

Therefore this paper aims to solve the correlated WMP model for the same experimental data studied by Miguel *et al.* (2016) with the Simulated Annealing algorithm method implemented in Python language and compare both results.

2. METHODOLOGY

2.1 The WMP model

The WMP model consists of modelling the flame as an array of point sources which emit radiation in different intensities, describing the same radiation profiles obtained experimentally. These point sources are distributed on the flame axis and emit radiation in every direction with the same intensity. Figure 1 shows a graphical representation of the WMP model.

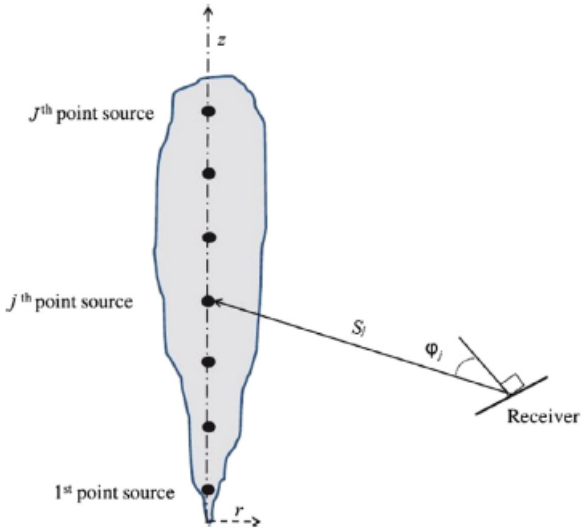

Figure 1: Representation of the WMP model. Adapted from Hankinson and Lowesmith (2012)

The formulation of the WMP model states that the radiation flux detected by a receiver far a certain distance from the flame is given by:

$$q''_R = \sum_{j=1}^{J} q''_j = \sum_{j=1}^{J} \frac{w_j X_R \dot{m} LHV \tau_j}{4\pi S_j^2} \cos\varphi_j \tag{1}$$

where q''_R is the radiation flux received from the j^{th} point source (with $1 \leqslant j \leqslant J$), w_j is the weight of the j^{th} point source, $\dot{m}$ is the fuel mass flow rate, LHV is the lower heating value of the fuel, τ_j is the transmissivity of the medium over the distance S_j (assumed as 1, since air can be considered a non participating medium in the near-field), and φ_j is the angle between the radiation path from the j^{th} source and the normal vector of the receiver surface. The fraction of radiative heat X_R can be approximated by experimental measurements and is given by:

$$X_R = \frac{Q_R}{Q_f} = \frac{\int_{-\infty}^{+\infty} q''_R 2\pi R dz}{\dot{m} LHV} \tag{2}$$

Since the total energy emitted by the flame must remain constant regardless of the number of source points used to model, it follows that:

$$\sum_{j=1}^{J} w_j = 1 \tag{3}$$

Despite being able to offer good predictions of the radiation profile in the near field, values calculated for distances too close to the flame cannot be considered as correct, since spatial effects from the flame envelope start to become meaningful. Moreover the envelope circles the flame axis with a radius of nearly $0.17 \times L_f$, invalidating completely the model for distances near this value. The way the problem is formulated implies that different values of w_j can be used to obtain the same answer, or at least the same level of accuracy. Hankinson and Lowesmith (2012) proposed a two-step linear variation of these values, given by:

$$w_j = jw_1 \tag{4a}$$

$$w_j = \left[j_p - \frac{j_p - 1}{J - j_p + 1} \cdot (j - j_p + 1) \right] \cdot w_1 \tag{4b}$$

where j_p is the position of maximum weight, suggested as $0.75 \times J$. In this case, the sources were uniformly distributed along the visible length of the flame, but other configurations of position and weights could be found to better satisfy the experimental data. Since this formulation offers the possibility of multiple answers to the same outcome, it is useful to search for a correlation based on the flame parameters to guide the calculation of these variables.

2.2 The inverse problem

In order to find a suitable correlation to describe the behaviour of the involved variables, the problem was formulated as an inverse problem, with an objective function to be minimised. Miguel *et al.* (2016) formulated the objective function F_o given by:

$$F_o(X_R, w_j) = \left[\sum_{i=1}^{I} (q''_{R,m,i} - q''_{R,i})^2 \right]^{1/2} \tag{5}$$

where *I* is the number of measurement points, $q''_{R,m,i}$ is the radiative flux measured in each point and $q''_{R,i}$ is the calculated radiative flux in the same point. In order to guarantee that equation (3) is satisfied, an auxiliary variable D_j is defined, such that:

$$w_j = \frac{D_j}{\sum_{j=1}^{J} D_j} \tag{6}$$

Besides that, it was also analysed a deviation index γ defined by:

$$\gamma_i = \frac{|q''_{R,m,i} - q''_{R,i}|}{\max_i(q''_{R,m,i})} \times 100\% \tag{7}$$

Miguel *et al.* (2016) proposed these expression for the same configuration proposed by Hankinson and Lowesmith (2012), with the weights uniformly distributed along the flame axis, only a distribution length L_s was used, defined as:

$$L_s = \beta L_f \tag{8}$$

where β is a scale factor. The positions of the weights are calculate as following:

$$\Delta z = L_s / J \tag{9a}$$

$$z_1 = \Delta z / 2 \tag{9b}$$

$$z_j = z_{j-1} + \Delta z \tag{9c}$$

where z_j is the height of the source measured from the burner outlet.

This formulation has $V = J + 1$ variables to be solved, that is, X_R and each one of the J auxiliary parameters D_j. Since the weights are considered completely independent between them, following no correlation at all, several combinations of values can be found to satisfy the same final result of F_o. For this reason, Miguel *et al.* (2016) proposed a quadratic correlation for X_R and w_j, functions of the normalised flame heat release rate q_f, given by the following expressions:

$$q_f = Q_f / Q_{ref} \tag{10a}$$

$$X_R(q_f) = A_{X_R} q_f^2 + B_{X_R} q_f + C_{X_R} \tag{10b}$$

$$D_j(q_f) = A_j q_f^2 + B_j q_f + C_j \tag{10c}$$

In this work it was considered $Q_{ref} = 1$ kW/m^2.

This way it is possible to correlate the evolution of the needed parameters with the flame behaviour when its heat release rate is increased or decreased. The global objective function, considering data from all F flames measured, now can be written as:

$$F_o(A_j, B_j, C_j, A_{X_R}, B_{X_R}, C_{X_R}) = \left[\sum_{f=1}^{F} \sum_{i=1}^{I} (q''_{R,m,i} - q''_{R,i})^2 \right]^{1/2} \tag{11}$$

The choice for a quadratic equation is completely arbitrary and could be changed in future works.

Applying those correlations can help to achieve more knowledge of the phenomenon, but computationally it increases threefold the number of variables to solve ($V = 3 \times (J + 1)$), since each one of the variables in the previous formulation is now associated with a quadratic equation dependent of 3 coefficients. The large quantity of variables makes it harder to find an optimal solution. To help with this problem there is a large range of methods, many of them using stochastic approaches. Miguel *et al.* (2016), for instance, used the Generalised Extremal Optimisation, or GEO, which manipulate the variables as one single binary string and evaluates their fitness as each bit mutates. However the GEO needs to impose a resolution in order to convert real values to binary numbers, thus filtering the objective function at some level. In order to assess the differences between methods and check if there is any improvement, in this paper it will be used the Simulated Annealing algorithm.

2.3 Simulated Annealing algorithm

The Simulated Annealing algorithm gains its name for being an analogy to the process of annealing applied to metals to increase its ductility and to allow them to be easier to work with. The SA algorithm was presented by Kirkpatrick *et al.* (1983) applied to project of electronic systems, and is based on statistical thermodynamic theory.

In the real phenomenon, the annealing process consists in heating a hard piece of metal (usually one that has passed by a process of quenching or hardening) until the point of austenitization, allowing the molecules to adjust their bonds to a higher level of energy while keeping it in the solid state, thus increasing its malleability. This is just possible because the higher temperature makes these molecules vibrate more, allowing them to "test" more arranging possibilities and eventually stay in those that lowers the overall energy level. In order for this process to work, the temperature must be maintained for a certain period of time and the cooling must be slow enough to ensure that the molecules will be permitted to "choose" the best orientation. If for some reason the temperature is steeply decayed, the molecules will take the immediately most favourable position, which is usually not the best, and the material will be quenched.

According to statistical thermodynamics, the probability of a molecule to be in a certain level of energy is given by the Boltzmann distribution:

$$P(\varepsilon_i) = \frac{\exp^{\frac{-\varepsilon_i}{kT}}}{\sum_{j=1}^{m} \exp^{\frac{-\varepsilon_j}{kT}}} \tag{12}$$

where ε_i is the energy of state i, k is the Boltzmann constant, T is the thermodynamic temperature and m is the total number of states of the system.

The algorithm does an analogy interpreting a candidate solution $\vec{X}$ as a state, the value of the objective function F_o as the energy level and setting a parameter T to simulate the cooling process. The SA pseudocode can be written as showed in Fig. 2. The nomenclature used is:

- $\{x\}$ is the current solution;
- $\{x^*\}$ is the best solution found;
- F_o is the objective function;
- T_0 is the initial temperature;
- T is the current temperature;
- p' is a random real number between 0 and 1;
- $\{r\}$ is a random real vector of components between -1 and 1 with the same size as $\{x\}$;
- v is the perturbation magnitude.

Simulated Annealing pseudocode

Generate an initial solution $\{x_0\}$;
Make $\{x\} = \{x_0\}$ and $\{x^*\} = \{x_0\}$;
Make $T = T_0$;
while *conditions* = FALSE **do**
    Chose solution $\{x'\} = \{x\} + v \cdot \{r\}$;
    Calculate $\varepsilon = F_o(\{x'\}) - F_o(\{x\})$;
    if $\varepsilon < 0$
        Make $\{x\} = \{x'\}$;
        if $F_o(\{x'\}) < F_o(\{x^*\})$
            Make $\{x^*\} = \{x'\}$;
        end
    else
        Generate p';
            if $p' < \exp^{-\varepsilon/T}$;
                Make $\{x\} = \{x'\}$;
            end
    end
    Calculate acc;
    Refresh value of v;
    Refresh value of T;
end
Return final value of $\{x^*\}$.

Figure 2: Pseudocode for the Simulated Annealing algorithm. Adapted from Silva Neto *et al.* (2016).

- acc is the acceptance rate, defined as $acc = N_{acc}/N_s$, where N_s is the number of iterations sampled and N_{acc} is the number of accepted iterations.

The value of v is changed in order to keep the $acc \approx 50\%$: when acc is low, it means that the step is too large and probably there are no better solutions in the domain, so v is decreased to explore locally; when acc is to high, it means the steps are too small and the algorithm is performing almost a gradient descent, so v is increased to explore globally and make sure that the program is not stuck in a local minimum.

The function that controls the descent of T must allow initially a broad exploration of the domain, since low temperatures reduce the probability of acceptance of a locally worse solution, and thus the change of region to be explored.

The functions that control v and T can be defined depending of the problem studied. In fact, the most difficult task to ensure the adequate algorithm running is the setting of these parameters and functions. Despite that, when well established, the SA shows itself robust to find the global minimum.

2.4 Coordinate Descent

A final refinement phase was added after the SA algorithm was finished, to improve the result inside the convex region where the best solution so far was located. The method of coordinate descent was used for it, which consists in test each direction parallel to each axis of the search space and then follow the one that presents the best variation (in a minimisation problem, the direction with the steeper downward slope) until it reaches a worse result again (it is, the slope becomes upward). Then the algorithm checks every direction again, and repeats the process until all directions present an unfavourable slope, which means that the best result inside that region (convex for minimisation or concave for maximisation) was found. This method have the advantage over the traditional gradient descent for not having the need to calculate the derivative or follow directions that are not parallel to any axis, allowing a faster calculation. Besides that, a good implementation of SA before the coordinate descent helps to keep low the number of iterations needed for refinement.

2.5 Experimental setup

Radiative heat flux distributions are measured for non-premixed methane flames in an air coflow burner. The burner is constructed to match the one presented in Santoro *et al.* (1983), which has a central tube with 11.1 mm i.d. inside of a coflow annulus with 101.6 mm. Measurements under the injector exit are allowed by the increasing of the length of the injector from 4 mm to 60 mm over the coflow exit. The standard Santoro burner has a ceramic honeycomb at the air exit, which was not used for these experiments.

The measurements were taken for 12 flames of methane with different heat power, from 0.1386 kW to 0.5545 kW

Table 1: Measured flames used in this work and in the work by Miguel *et al.* (2016)

Flame	Q_f [kW]	L_f [m]	R [m]	I
1	0.139	0.046	0.054	19
2	0.166	0.055	0.054	20
3	0.194	0.066	0.054	20
4	0.222	0.076	0.054	20
5	0.250	0.088	0.054	21
6	0.277	0.102	0.054	22
7	0.277	0.101	0.114	28
8	0.333	0.126	0.114	19
9	0.388	0.139	0.114	20
10	0.444	0.166	0.114	20
11	0.499	0.176	0.114	21
12	0.554	0.189	0.114	21

($\dot{m}\times$50,016 kJ/kg). The dry air coflow velocity was made constant (0.210 m/s) for all flames. The flow rates were controlled and measured with electronic mass flow meters. The flames heat powers are presented in Tab. 1. The radiative heat fluxes were measured with a MEDTHERM heat flux transducer model 64-0.5-20/ZnSeW-1C-150, which is a Schmidt-Boelter thermopile with a field of view of 150° with a ZnSe window. The window has a flat spectral transmissivity of 70% for a wavelength interval from 0.7 μm to 17 μm, the transducer has a coated face with flat spectral absorptivity along the electromagnetic spectrum. The uncertainty for this sensor is 3% of the reading signal for an interval of confidence of 95%. The sensor is displaced along the flame axis at a radial distance R, with the positions marked with a graduated scale. For each position, it is acquired a signal for the flame radiative heat flux and the background signal (without flame). Each signal is represented by a sampling of 50 acquisitions at 2.5 Hz. The fluxes uncertainty reported takes in account the uncertainties of the sensor signal, the acquisition system and the variance of the sample. The distance R and the limits of the displacing were taken to guarantee that the entire flame was within the sensor field of view. The visible flame lengths reported were visually determined from an average of 5 photographs with long exposure time calibrated with a graduated scale form flames under 0.2771 kW, for the flames with higher power, the visible flame length is the average length taken from 150 images with low exposure time.

2.6 Parameters

Since the main objective of this paper is to compare the application of the SA algorithm to the results presented by de GEO in the work of Miguel *et al.* (2016), the same constraints were used, that is:

$$\begin{cases} -5 \leq A_{X_R}, A_{D_j}, B_{X_R}, B_{D_j} \leq 5 \\ 0 \leq C_{X_R}, C_{D_j} \leq 10 \end{cases} \tag{13}$$

Similarly, the weights were uniformly distributed as described by Eq. (8), (9a), (9b) and (9c). Given that L_f changes for each flame, the absolute positions also vary, but the relative positions are kept the same.

It was defined a maximum number of iterations N and a number of iterations N_T in which the temperature is kept with its initial value T_0. For iterations after N_T, the temperature is set to decrease according to eq. 14:

$$T = T_0 f^{\frac{it - N_T}{N - N_T}} \tag{14}$$

Equation (14) is defined in such a way that at iteration N (that is, the last one), $T = fT_0$. The perturbation size v was defined as being the same to all variables, since they have the same order of magnitude. This should not be done if the variables belonged to different orders of magnitude, for a small step to one variable could be considered large to others. The value of v is corrected in accordance to Eq. (15):

$$\begin{cases} \alpha = \frac{acc-1}{45} + 1.01 & 0.55 < acc \\ \alpha = 1 & 0.45 \leq acc \leq 0.55 \\ \alpha = \frac{acc}{45} + 0.99 & acc < 0.45 \\ v' = \alpha v \end{cases} \tag{15}$$

where α is the multiplying correction factor and v' the new perturbation size.

Some preliminary tests showed instability in the increase or decrease of v which, depending on the initial conditions, could lead to errors in the algorithm, with values tending to zero or infinity. For this reason limits were imposed to v,

keeping it in the interval $10^{-3} \leq v \leq 5$. Moreover, when a perturbation reaches beyond one of the boundaries, the excess is reduced from the limit as if the variable "bounced" back to the domain.

It was also applied a penalty to the weight when any w_j is calculated as negative. In this case, it is imposed $w_j = 1000$, consequently making F_o to take very high values and making improbable the acceptance of that solution. This was done differently by Miguel *et al.* (2016), which considered $D_j = 0$ whenever D_j was negative. The different approach of this work is chosen because it avoids distortions in the final curve and guides the algorithm to find a neat correlation.

Table 2 brings all numeric values used as initial parameters.

Table 2: Initial parameters used in this work.

Parameter	Name	Value
J	Number of source points	$[2, 3, 4, \ldots, 12]$
β	Distribution length scale factor	$[1, 1.25, 1.5, \ldots, 2.5]$
T_0	Initial temperature	100
f	Temperature reduction factor	0.001
N	Total number of iterations	10^6
N_T	Number of iterations at T_0	$0.01N = 10^4$
N_s	Number of iterations to sample acc	$0.001N = 10^3$

3. RESULTS

It was studied the effect of different β and J combinations on F_o to find the best solution. Table 3 shows the statistical results for 50 runs.

The results show an average value of F_o close to the 0.5 kW/m^2 found by Miguel *et al.* (2016) for most combinations of parameters, ranging from 0.44 to 0.56 kW/m^2 approximately. There is a trend to decrease the average value of F_o as β increases. This behaviour is somewhat expected since there is radiation being emitted by hot gases after the visible length of the flame, so it is reasonable to consider that should exist one or more point sources of radiation in that region. Thus, the best values are found mainly in higher values of β (2.00, 2.25 and 2.50). Also, while analysing the table in respect to J, it can be observed that the best values of F_o for each β are concentrated in the middle of the table, for values of J around 5. It can be explained by the fact that a small quantity of point sources restricts too much the resultant radiation profile, thus leading to high values of F_o. Besides that, too many sources leads to a high number of variables, making it harder for the algorithm to find better solutions.

This second observation can also be demonstrated when standard deviations values are taken into account: the bottom right corner of the table, with higher values of both J and β, present larger σ, demonstrating the algorithm's increased uncertainty when dealing with many variables. The downside of it is that the method should be retuned for higher J, which would increase processing time because of the larger search domain. On the good side, a higher σ combined to a not so larger μ means there is a chance to find better results for these parameter combinations, if they are properly explored. The small values of σ for small values of both β and J ensure that those parameters are not the best suited to solve the correlated WMP problem inside the defined search space.

A clearer analysis combining data from μ and σ can give a better notion of the best region to be explored. Table 4 shows possible values when subtracting 2σ from μ, giving some sense of probability to find better results for each

Table 3: Mean values of F_o and standard deviations found for each combination of J and β in 50 runs.

	F_o [kW/m^2] - μ/σ						
J	$\beta = 1.00$	$\beta = 1.25$	$\beta = 1.50$	$\beta = 1.75$	$\beta = 2.00$	$\beta = 2.25$	$\beta = 2.50$
2	0.744/0.007	0.604/0.011	0.524/0.015	0.497/0.016	0.527/0.017	0.623/0.010	0.769/0.008
3	0.692/0.015	0.582/0.019	0.505/0.029	0.461/0.037	0.439/0.037	0.432/0.039	0.441/0.032
4	0.683/0.016	0.576/0.014	0.500/0.026	0.441/0.043	0.423/0.042	0.410/0.049	0.411/0.049
5	0.679/0.015	0.568/0.015	0.497/0.025	0.469/0.040	0.435/0.051	0.420/0.056	0.425/0.061
6	0.680/0.015	0.567/0.018	0.506/0.029	0.466/0.035	0.447/0.041	0.468/0.067	0.452/0.074
7	0.681/0.016	0.567/0.018	0.509/0.020	0.477/0.042	0.483/0.048	0.485/0.070	0.478/0.093
8	0.683/0.015	0.568/0.018	0.521/0.022	0.491/0.047	0.500/0.072	0.495/0.081	0.524/0.118
9	0.682/0.014	0.572/0.016	0.522/0.023	0.508/0.045	0.521/0.056	0.529/0.100	0.569/0.120
10	0.687/0.013	0.570/0.014	0.520/0.025	0.502/0.036	0.522/0.072	0.556/0.095	0.599/0.122
11	0.690/0.013	0.573/0.015	0.524/0.025	0.518/0.047	0.561/0.093	0.602/0.122	0.634/0.147
12	0.690/0.011	0.571/0.012	0.524/0.031	0.540/0.055	0.556/0.081	0.617/0.128	0.708/0.162

Table 4: Values of F_o deviated 2σ to the left from the mean value μ for each combination of J and β in 50 runs.

F_o [kW/m^2] - $\mu - 2\sigma$							
J	$\beta = 1.00$	$\beta = 1.25$	$\beta = 1.50$	$\beta = 1.75$	$\beta = 2.00$	$\beta = 2.25$	$\beta = 2.50$
2	0.731	0.582	0.494	0.464	0.493	0.602	0.752
3	0.662	0.544	0.446	0.387	0.364	0.354	0.376
4	0.650	0.548	0.447	0.356	0.338	0.312	0.314
5	0.650	0.538	0.447	0.389	0.332	0.309	0.304
6	0.651	0.532	0.449	0.395	0.364	0.334	0.304
7	0.648	0.531	0.469	0.393	0.387	0.346	0.291
8	0.653	0.531	0.477	0.398	0.356	0.333	0.288
9	0.654	0.540	0.476	0.419	0.408	0.329	0.329
10	0.661	0.543	0.470	0.431	0.378	0.366	0.355
11	0.663	0.543	0.474	0.423	0.375	0.357	0.339
12	0.667	0.548	0.461	0.430	0.393	0.362	0.385

combination.

As confirmed by Table 4, the use of low β values is surely not suited for this problem, while high β values have more chance to give better results. As discussed before, probably because of the chosen algorithm parameters the best chances to find a good F_o value are found in intermediate values of J, the best value being shown by the combination $\beta = 2.5$ and $J = 8$ ($\mu - 2\sigma = 2.88$ kW/m^2). This behaviour also implies that, besides retuning the algorithm for larger number of variables, larger values of β should also be explored in future works, up to the point results start to loose quality, finding the probable best region to explore the problem. From the total 3850 final results of F_o, 2 (0.05%) were under 0.3 kW/m^2, 251 (6.52%) under 0.4 kW/m^2, 1346 (34.96%) under 0.5 kW/m^2 and 2879 (74.78%) under 0.6 kW/m^2.

The iteration number (without counting the coordinate descent refinement phase) when the best solution was found was also recorded. Low values of β needed less iterations (around 830,000) but not much less than higher values (around 910,000). No clear trend was shown varying J for a fixed β. Standard deviations of this parameter also showed no meaningful pattern.

The best value found in all 50 runs was encountered with $J = 8$ and $\beta = 2.25$, presenting a value of $F_o = 0.283$ kW/m^2, almost half the one brought by Miguel *et al.* (2016). The values of $\gamma_{avg} = 3.39\%$ and $\gamma_{max} = 12.6\%$ are larger than those found by Miguel *et al.* (2016) (8.6% and 2.9%, respectively), which shows that not for every case a better F_o means less γ, due to their different approach in calculation (F_o makes the sum of the squares and then takes the square root, thus giving more weight to distant points as they deviate further from experimental data; γ is calculated by the arithmetic mean, so points have a more uniform influence on the final result). Still it is valid to note that Miguel *et al.* (2016) found the best case for the same β and just one source point less than this work. This fact shows consistency between both methodologies and increases trust in the previous results. Table 5 brings the coefficients found for the best result and Figure 3 brings the resultant profiles calculated from those coefficients.

Figure 3 shows good agreement between experimental and calculated data. Interestingly, the coefficients that calculate X_R do not follow those found by a least squares approximation (which are $A_{X_R} = -0.406$, $B_{X_R} = 0.394$ and $C_{X_R} = 0.071$), meaning that the coefficients found for each D_j compensated the difference of those for X_R without damaging the result, evidencing flexibility in the formulation. Some of the coefficients exhibited in Table 5 show values in the border of the domain ($A_2, A_8, B_2, B_3, B_6, C_{X_R}$ and C_7), suggesting that better results probably lay just beyond the defined limits. Further explorations, whatever the method used, should take into consideration the enlargement of these limits.

Factors that need still to be explored include the comparison to other deterministic and stochastic methods aiming to

Table 5: Values found for A, B and C coefficients for the best case calculated, $J = 8, \beta = 2.25$.

	A	B	C
X_R	-0.989470	0.876744	0.000000
D_1	0.052589	3.157173	4.009633
D_2	5.000000	5.000000	4.723760
D_3	2.327534	5.000000	3.134119
D_4	2.851970	-4.070759	3.821287
D_5	-1.190367	-4.552135	2.920846
D_6	-0.123265	-5.000000	2.839595
D_7	0.680776	-0.081263	0.000000
D_8	-5.000000	-3.440055	3.463280

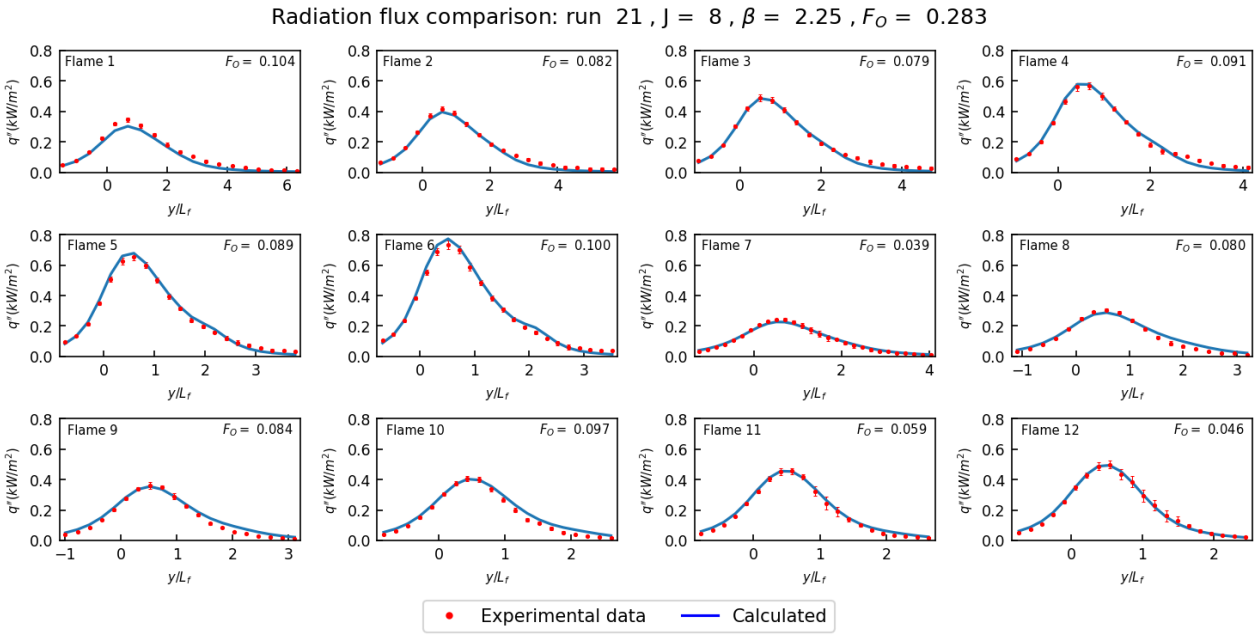

Figure 3: Resultant radiation profiles obtained from the coefficients shown in Table 5.

find the global minimum and the best correlations for engineering practice. Different approaches of objective functions and application of swarm intelligence could be interesting experiments. Also there can be made studies with a broader coverage of flames, varying flow, fuel and dilution parameters, for example.

4. CONCLUSIONS

Parameters of the correlated WMP model for flame radiation profile were optimised with the Simulated Annealing (SA) algorithm in Python language for a set of experimental data from methane diffusion flames, with a final refinement using the coordinate descent method. The results were then compared to those presented by Miguel *et al.* (2016), in which the GEO was the chosen optimisation method. Using the same formulation, 77 initial cases were run 50 times, and the results were analysed by their average and standard deviation values. The SA algorithm showed good results with similar average values of objective function than Miguel *et al.* (2016), but with standard deviations that show the possibility to find better results for high values of β and J. The best results were found for $J = 8$ and $\beta = 2.25$, giving $F_o = 0.283$ kW/m^2 and $\gamma_{avg} = 3.39\%$. Suggestions of future works are to test other deterministic and stochastic methods to solve the correlated WMP problem aiming to have more knowledge about the behaviour of the objective function and to verify if there is a global minimum with certainty. It will be also needed to be explored a broader range of flames varying combustion and flow regime.

5. ACKNOWLEDGEMENTS

BHS thanks CAPES (Brazil) due to its financial support by means of a Master's Degree Scholarship. FHRF thanks CNPq for research grants 309961/2013-0 and 476490/2013-8. All authors thank Petrobras S.A. for the financial support.

6. REFERENCES

Erchiqui, F., 2018. "Application of genetic and simulated annealing algorithms for optimization of infrared heating stage in thermoforming process". *Applied Thermal Engineering*, Vol. 128, pp. 1263–1272.

Fang, L., Zuo, H., Pang, L., Yang, Z., Zhang, X. and Zhu, J., 2018. "Image reconstruction through thin scattering media by simulated annealing algorithm". *Optics and Lasers in Engineering*, Vol. 106, pp. 105–110.

Hankinson, G. and Lowesmith, B.J., 2012. "A consideration of methods of determining the radiative characteristics of jet fires". *Combustion and Flame*, Vol. 159, pp. 1165–1177.

Holland, J.H., 1975. *Adaptation in natural and artificial systems*. Ann Arbor: Michigan University Press, Ann Arbor, Michigan, USA, 1st edition.

Kennedy, J. and Eberhart, R.C., 1995. "Particle swarm optimization". In *Proceedings of the IEEE International Conference on Neural Networks*. pp. 1942–1948.

Kirkpatrick, S., Gelatt, C.D. and Vecchi, M.P., 1983. "Optimization by simulated annealing". *Science*, Vol. 220, pp.

671–680.

Lucic, P. and Teodorovic, D., 2001. "Bee system: modelling combinatorial optimization transportation engineering problems by swarm intelligence". In *Preprints of the TRISTAN IV Triennal Symposium on Transportation Analysis*. pp. 441–445.

Miguel, R.B., Machado, I.B., Pereira, F.M., Pagot, P.R. and França, F.H.R., 2016. "Application of inverse analysis to correlate the parameters of the weighted-multi-point-source model to compute radiation from flames". *International Journal of Heat and Mass Transfer*, Vol. 102, pp. 816–825.

Santoro, R.J., Semerjian, H.G. and Dobbins, R.A., 1983. "Soot particle measurements in diffusion flames". *Combustion and Flame*, Vol. 51, pp. 203–218.

Silva Neto, A.J., Becceneri, J.C. and Campos Velho, H.F., 2016. *Inteligência computacional aplicada a problemas inversos em transferência radiativa*. EdUERJ, Rio de Janeiro, 1st edition.

Wei, L., Zhang, Z., Zhang, D. and Leung, S.C.H., 2018. "A simulated annealing algorithm for the capacitated vehicle routing problem with two dimensional loading constraints". *European Journal of Operational Research*, Vol. 265, pp. 843–859.

7. RESPONSIBILITY NOTICE

The authors are the only responsible for the printed material included in this paper.